

Shoot structure, light interception, and distribution of nitrogen in an *Abies amabilis* canopy

PAULINE STENBERG,¹ HEIKKI SMOLANDER,² DOUGLAS SPRUGEL³ and SAMPO SMOLANDER⁴

¹ Department of Forest Ecology, P.O. Box 24, FI-00014 University of Helsinki, Finland

² The Finnish Forest Research Institute, Suonenjoki Research Station, FI-77600 Suonenjoki, Finland

³ College of Forest Resources, AR-10, University of Washington, Seattle, WA 98195, USA

⁴ Department of Biosciences, Division of Genetics, P.O. Box 56, FI-00014 University of Helsinki, Finland

Received January 5, 1998

Summary We studied the effects of variation in shoot structure and needle morphology on the distributions of light and nitrogen within a Pacific silver fir (*Abies amabilis* (Dougl.) Forbes) canopy. Specifically, we investigated the role of morphological shade acclimation in the determination of resource use efficiency, which is claimed to be optimal when the distribution of nitrogen within the canopy is directly proportional to the distribution of intercepted photosynthetically active radiation (PAR). Shoots were collected from different heights in the crowns of trees representing four different size classes. A new method was developed to estimate seasonal light interception (SLI, intercepted PAR per unit needle area) of the shoots using a model for the directional distribution of above-canopy PAR, measurements of shoot silhouette area and canopy gap fraction in different directions. The ratio SLI/SLI_0 , where the reference value SLI_0 represents the seasonal light interception of a spherical surface at the shoot location, was used to quantify the efficiency of light capture by a shoot. The ratio SLI/SLI_0 doubled from the top to the bottom of the canopy, mainly as a result of smaller internal shading in shade shoots than in sun shoots. Increased light-capturing efficiency of shade shoots implies that the difference in intercepted light by sun shoots versus shade shoots is much less than the decrease in available light from the upper to the lower canopy. For example, SLI of the five most sunlit shoots was only about 20 times greater than the SLI of the five most shaded shoots, whereas SLI_0 was 40 times greater for sun shoots than for shade shoots. Nitrogen content per unit needle area was about three times higher in sun needles than in shade needles. This variation, however, was not enough to produce proportionality between the amounts of nitrogen and intercepted PAR throughout the canopy.

Keywords: morphological acclimation, Pacific silver fir, resource use efficiency.

Introduction

Several theories exist on how structure and function in plant canopies should be organized to optimize the utilization of

resources such as light, water, and nutrients (Verhagen et al. 1963, Kuroiwa 1970, Horn 1971, Mooney and Gulmon 1979, Field 1983, Bloom et al. 1985, Evans 1989, Farquhar 1989, Chen et al. 1993). These theories produce different solutions depending on the assumptions and constraints the optimization is based on.

Early theories showed that if the parameters of the light response curve do not vary with position in the canopy, photosynthesis is optimized if light interception per unit leaf area is constant throughout the canopy (Verhagen et al. 1963). This optimization is generally unachievable because upper leaves inevitably shade lower leaves, although it can be counteracted to some extent by differences in leaf angle (Miller 1967, Kuroiwa 1970, Horn 1971) and shoot structure (Sprugel 1989, Leverenz and Hinckley 1990, Sprugel et al. 1996, Stenberg 1996).

Other theories are based on the observation that the photosynthetic capacity of leaves (expressed as maximum CO_2 uptake per unit mass) is often proportional to their nitrogen concentration (Field and Mooney 1986). Given this, it can be shown that resource use is optimized when the distribution of nitrogen within the canopy is directly proportional to the distribution of intercepted PAR, when both are expressed on an area basis (e.g., Farquhar 1989). Many plant canopies have now been studied from this perspective (Field 1983, Hirose et al. 1989, Hollinger 1989, Ellsworth and Reich 1993, Evans 1993, Kull and Niinemets 1993), and in nearly all cases, it has been found that nitrogen per unit leaf area varies in parallel with light availability, although it rarely decreases sharply enough to remain proportional to light at lower levels of the canopy. However, these theories do not specify the physiological or morphological mechanism by which an optimal distribution is obtained, and structural variations above the level of the leaf have rarely been considered. Many common morphological and physiological adaptations to shade are in general agreement with an efficient use of resources, but quantitative estimates of their combined effects on, for example, canopy photosynthesis, are largely missing.

Acclimation responses causing variation in the physiology and morphology of leaves in different light environments greatly increase the complexity, but also the flexibility, of resource use optimization. Morphological adaptations in conifers include increases in specific needle area (SNA) and the ratio of shoot silhouette area to needle area with shading (e.g., Leverenz and Hinckley 1990, Niinemets and Kull 1995, Stenberg et al. 1995, Sprugel et al. 1996). The ratio of shoot silhouette area to needle area is referred to as STAR or SPAR, depending on whether total needle surface area or projected needle area is used in the denominator, respectively. The increase in STAR (SPAR) at lower irradiances reduces the variation in intercepted light per unit needle area of shoots in different parts of the canopy (Stenberg 1996). The simultaneous increase in SNA further diminishes the differences in light interception per unit needle mass or unit nitrogen.

These adaptations are in qualitative agreement with the theory by Farquhar (1989) stating that resource use is optimized when the distribution of photosynthetic capacity and nitrogen is proportional to the distribution of intercepted light (see Sprugel et al. 1996). However, to estimate the effects of acclimation in a canopy it is necessary to quantify the degree to which changes in SNA and SPAR modify the distribution of light and nitrogen. To do this, variations in nitrogen concentration, SNA and SPAR along the entire light gradient in the canopy must be described. The effects of variations in SPAR and SNA on the distribution of intercepted light within a canopy must also be quantified. It is a complicated problem because leaf and shoot morphology do not solely affect the photosynthetic properties of the leaf (shoot) itself, but change the whole profile of light in the canopy. In addition, because the shoot silhouette area varies with the direction of radiation (sun angle), it is not obvious how best to quantify light interception by a coniferous shoot.

We examined changes in SNA, SPAR and nitrogen concentration in Pacific silver fir (*Abies amabilis* (Dougl.) Forbes) with shading, and analyzed the implications of these changes on the distribution and utilization of light and nitrogen within the canopy. Special efforts were made to produce accurate estimates of seasonal light interception by the shoots, based on measurements of canopy transmittance and shoot silhouette area from many different angles.

Material and methods

In situ measurements

Measurements were made in a 37-year-old *A. amabilis* stand at 1200 m elevation in the Findley Lake research area about 65 km southeast of Seattle, WA (47°20' N, 121°35' W). We collected 47 current-year shoots (30 in 1994 and 17 in 1995) from the tips of branches at different heights in the crowns of eight trees. Tree height ranged from 2.4 to 8.6 m, and shoots were collected from two trees of each of the size classes: suppressed (< 4 m), intermediate (4–6 m), codominant (6–8 m), and dominant (≥ 8 m). Data were split into two categories, one comprising shoots from codominant and domi-

nant trees (29 shoots), and the other comprising shoots from suppressed and intermediate trees (18 shoots).

Shoot position and orientation were recorded before removing the shoots. The orientation of a shoot was determined by the inclination and azimuth of the shoot axis, and the shoot's rotation angle to the vertical. To define the rotation angle, we picture a vector (r) perpendicular to the hypothetical plane dividing the shoot into upper and lower sides, and pointing toward the shoot's upper side. We measured the angle of r to the vertical plane through the shoot axis, and attached to it a positive or negative sign depending on the opening direction. The positive opening direction of r is clockwise when the tip of the shoot is pointing toward the viewer.

After the sample was collected, we took a hemispherical photograph at each shoot location with a Nikon 8-mm lens and Kodachrome 200 film. These photographs were analyzed with the CANOPY hemispherical photo analysis program (Rich 1989). The program provided the fraction of gaps separately for 18 inclination bands (width 5°) and eight azimuths (width 45°) (144 different sky sections) as well as total canopy openness, defined as the unweighted fraction of open sky (indirect site factor according to Anderson (1964) and Rich (1989)).

Mathematically, canopy openness is defined as:

$$\text{OPENNESS} = \frac{1}{2\pi} \int_{\Omega} \text{gf}(\omega) d\omega, \quad (1)$$

where Ω represents the upper hemisphere and $\text{gf}(\omega)$ the gap fraction in the direction ω of the sky.

Measurement of shoot morphology and silhouette area

The directional distribution of shoot silhouette area (SSA) was produced by measuring SSA photographically in different view directions (ϕ , γ) and constructing spline functions to interpolate smoothly between the measured values (bicubic spline interpolation; see Press et al. 1992). The silhouette areas were measured with a digital camera attached to an image analysis system (OPTIMAS, BioScan Inc., Edmonds, WA). The focal length of the lens (AF Nikkor) was 180 mm, and the distance between shoot and camera was 7.0 m for long shoots and 4.2 m for small shoots. The maximum view angle of the shoot was 1.5°. The system was calibrated according to the manufacturer's specifications for each measurement distance.

Following earlier practice (Oker-Blom and Smolander 1988), we define the inclination angle (ϕ) as the angle of the shoot axis to the plane of projection. Thus, for $\phi = 0^\circ$, the shoot axis is perpendicular to the direction of view (camera), and for $\phi = \pm 90^\circ$, the shoot axis is parallel to the direction of view. The value of ϕ is positive when the branch tip is pointing toward the viewer, and negative when the branch tip is pointing away from the viewer. The rotation angle (γ) is defined as the angle between the vector (r) and the plane going through the shoot axis and the view direction. Thus, when $\gamma = 0^\circ$, the shoot's upper side is facing the viewer, and when $\gamma = \pm 90^\circ$, the shoot is viewed from the side (see Figure 1).

A set of measurements was made where the rotation angle (γ) was held fixed and the inclination angle (ϕ) was changed in

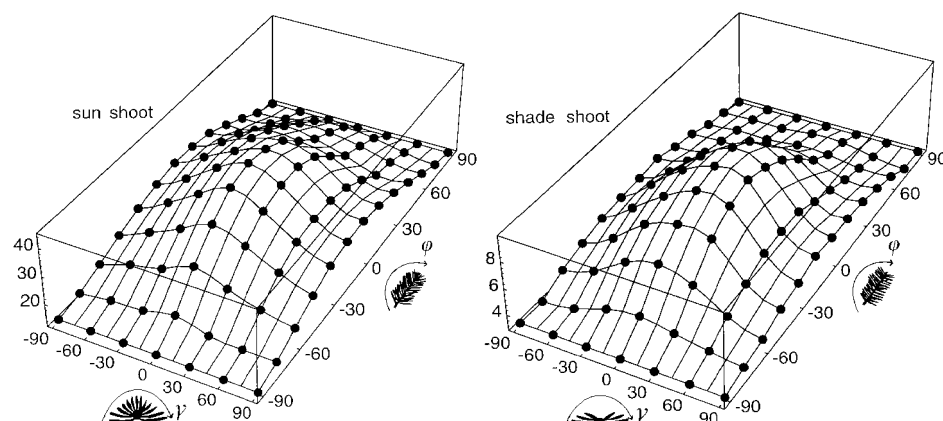


Figure 1. Directional distribution of SSA (cm^2) of a sun shoot and a shade shoot. The shoot is assumed to lie on its flat side, and the branch tip points to the positive ϕ -axis. The \bullet denotes a measured value. Note the different scales on the vertical axes for the sun (left) and shade shoots.

equal steps. This procedure was then repeated after changing the rotating angle in equal steps. In the 1994 measurements, the inclination and rotation angles were both changed in steps of 45° , giving a total of 16 silhouette areas measured per shoot. In 1995, the inclination angle was changed in steps of 15° , and the rotation angle was changed in steps of 30° , giving 72 silhouette areas measured per shoot. Interpolation surfaces for SSA of a “sun” shoot (canopy openness = 0.746) and a “shade” shoot (canopy openness = 0.130) are shown in Figure 1.

After measurement of shoot silhouette area, needles were detached from the shoot and the projected area of all needles on the shoot (PNA_s) was measured photographically with the OPTIMAS-system, equipped with a lens with a focal length of 50 mm (see Kershaw and Larsen 1992). The silhouette to projected leaf area ratio (SPAR) was obtained by dividing SSA by PNA_s . The ratio of $\text{SSA}(0,0)$ to PNA_s is referred to as SPAR_{\max} , although SSA does not necessarily attain its maximum value at $\phi = \gamma = 0$ (Figure 1). The mean of SSA taken over all directions of the sphere ($\overline{\text{SSA}}$) was obtained by calculating the mean of the spline function constructed to describe SSA in all directions. The value of $\overline{\text{SSA}}$ divided by PNA_s yields the spherically averaged silhouette area ratio ($\overline{\text{SPAR}}$).

We also measured shoot length, number of needles per shoot, mean needle length and thickness, and needle dry weight (48 h at 70°C). The nitrogen content of needles was measured with a LECO CHN-900 analyzer (LECO Co., St. Joseph, MI) (Table 1).

Simulation of above-canopy and within-canopy distributions of PAR

Incoming PAR was simulated by a method similar to that described by Stenberg (1996), but taking into account the azimuthal direction of the sun also. The period from June 1 to October 1 was chosen to represent the growing season at the study site. Input assumptions and parameters for the simulation model were as follows: (1) the amount of PAR available at the top of the atmosphere (the PAR equivalent of the solar constant) was assigned the value of 600 W m^{-2} (Weiss and Norman 1985); (2) it was assumed that 61% of the PAR incident on a horizontal surface at the top of the atmosphere is received at the ground (Western Solar Utilization Network 1980); (3) of the penetrated PAR, 55% entered as direct radia-

tion, and 45% as diffuse sky radiation (Fritschen and Hsia 1979) (Assumptions 1–3 fixed the seasonal amount of incoming PAR per unit horizontal surface (Q_h) at 1203 MJ m^{-2} , of which the direct and diffuse components were 662 MJ m^{-2} and 541 MJ m^{-2} , respectively); (4) the directional distribution of sunlight was produced by assuming that clear sky conditions prevailed throughout the season, and transmittance of the atmosphere to direct radiation was set to 0.73 in the zenith direction, and was corrected for atmospheric path length. The distribution obtained in this way was then multiplied by a factor (< 1) to give the “known” amount of direct PAR; and (5) the directional distribution of diffuse radiation was assumed to be isotropic.

The simulated distribution of PAR incident from different sections of the sky is shown in Figure 2. Total incoming PAR, expressed as the energy received per unit cross-sectional area of a spherical surface (Q_o), was 2109 MJ m^{-2} . The directional distribution of PAR around a shoot (Figure 3A) was obtained by multiplying each entry in the sky energy matrix (Figure 2A) by the corresponding entry in the hemispherical matrix (Figure 3B), containing the gap fractions in the 144 different sections of the sky.

Table 1. Structural characteristics and estimates of the light environment of the sample shoots.

| Characteristic | Range | Mean |
|---|-------------|-------|
| Shoot length (cm) | 2.2–15.7 | 7.7 |
| Needle density (cm^{-1}) | 8.5–28 | 18.1 |
| Needle area per shoot (cm^2) | 3.4–111.6 | 40.3 |
| Needle thickness (mm) | 0.25–0.88 | 0.54 |
| Needle length (mm) | 8–26 | 17.9 |
| SNA ($\text{cm}^2 \text{ g}^{-1}$) | 33.2–122.5 | 62.3 |
| N concentration (%) | 0.56–1.4 | 0.95 |
| N content (mg cm^{-2}) | 0.084–0.354 | 0.174 |
| $\overline{\text{SPAR}}$ | 0.262–0.561 | 0.359 |
| SPAR_{\max} | 0.337–0.993 | 0.556 |
| $\overline{\text{SSA}}$ /needle dry weight ($\text{cm}^2 \text{ g}^{-1}$) | 9.05–51.75 | 23.96 |
| Openness | 0.006–0.82 | 0.313 |
| SLI (kJ cm^{-2}) | 0.94–59.5 | 23.7 |
| SLI _o (kJ cm^{-2}) | 1.88–187 | 68.8 |
| SLI/SLI _o | 0.252–0.764 | 0.414 |

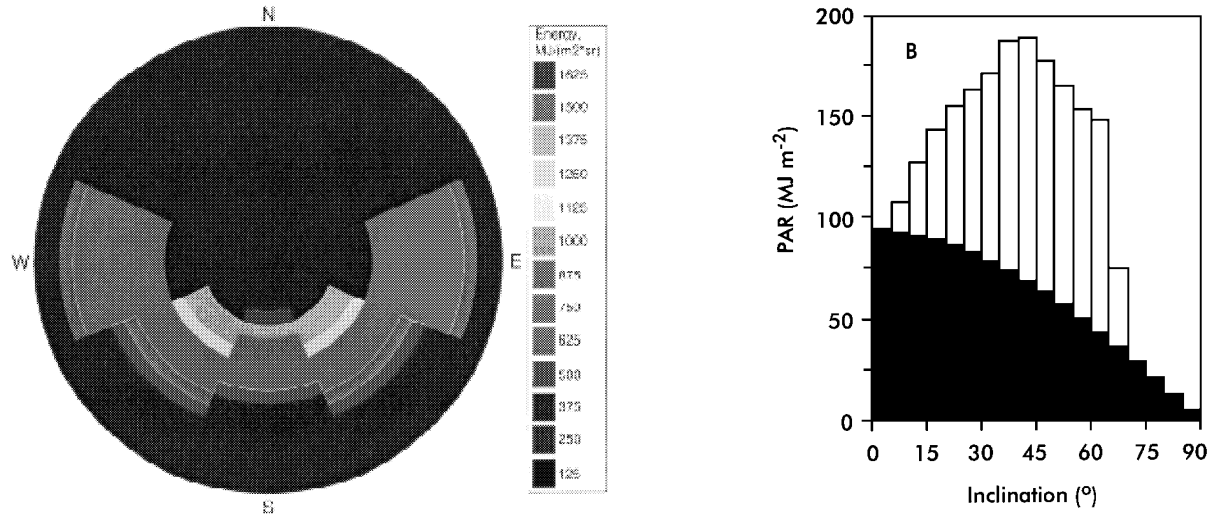


Figure 2. Simulated distributions of above-canopy PAR at the study site during the growing season. A. Sky energy matrix—the hemisphere is divided in 144 (18×8) sections, and the value (color) assigned to each section is the radiant energy per unit area incident from unit solid angle around that direction of the sky. Values shown on the scale correspond to the upper limits of the intervals. B. Division of direct (\square) and diffuse (\blacksquare) PAR into inclination bands.

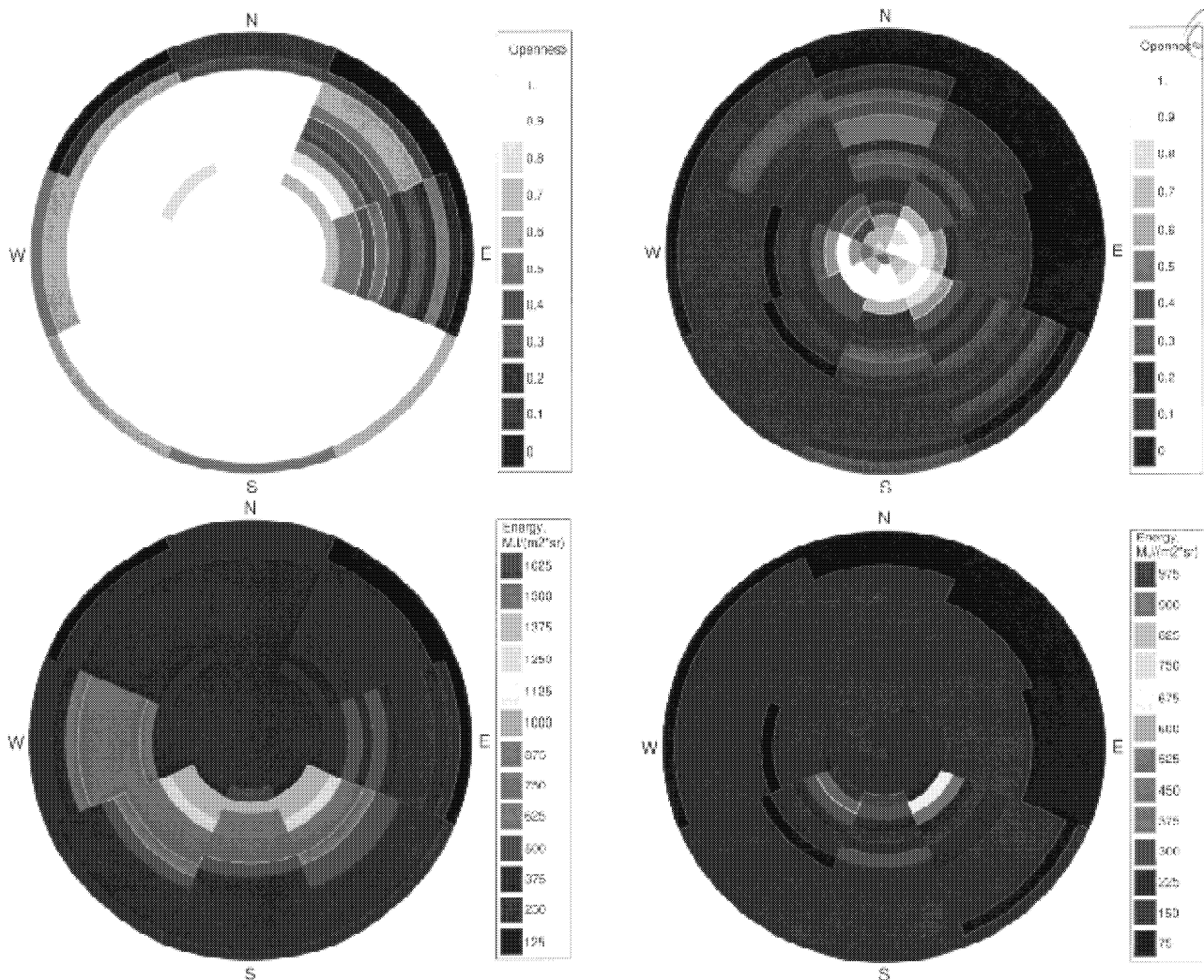


Figure 3. A. Canopy openness (digitized photographs), presented as a hemispherical matrix, at the location of a sun shoot (top left panel) and a shade shoot (top right panel). B. Hemispherical distribution of PAR at the shoot locations. Note the different scales for the top and bottom panels.

Estimation of light interception by the shoots

We define the seasonal light interceptance (SLI) of a shoot as the amount of PAR intercepted per unit projected leaf area of the shoot (PNA_s) during the growing season. Formally:

$$SLI = \int_{\Omega} q(\omega)gf(\omega)SPAR(\phi_{\omega}, \gamma_{\omega})d\omega, \quad (2)$$

where $q(\omega)$ is the seasonal amount of radiant energy (per unit area and solid angle) incident from the direction ω of the sky (see Figure 2A). The inclination angle (ϕ_{ω}) and rotation angle (γ_{ω}) (Equation 2) with respect to a given view direction (ω) vary with shoot orientation.

Equation 2 was numerically integrated by summation over the sky sections ($i = 1, \dots, 144$). The inclination (ϕ_i) and rotation (γ_i) angles corresponding to the direction from the midpoint of each section (i) were calculated based on the recorded information of the shoot's natural orientation in the canopy. Technically, this was done by transformation of the coordinate system (see Figure 1). The (interpolated) value of SSA(ϕ_i, γ_i) was then assigned to section (i).

The efficiency of light capture by a shoot was quantified by comparing SLI to the amount of PAR received per unit cross-sectional area of a spherical surface at the same location (SLI_o):

$$SLI_o = \int_{\Omega} q(\omega)gf(\omega)d\omega. \quad (3)$$

The SLI_o can be interpreted as a measure of the amount of available PAR at the shoot location, whereas SLI is the actual PAR intercepted by the shoot. We used the ratio of SLI to SLI_o to compare the relative efficiency of light capture by shoots in different parts of the canopy.

From Equations 2 and 3, it follows that if there is no directional variation in SSA (i.e., SPAR equals \overline{SPAR} in all directions), or if the shoot is surrounded by an isotropic radiation field ($q(\omega)gf(\omega)$ is constant), then $SLI/SLI_o = \overline{SPAR}$.

Results

The radiation regime

Because the directional distribution of diffuse sky radiation was assumed to be isotropic, differences in the amount of radiant energy from different sections of the sky result from the direct solar component (Figure 2A). The highest value (brightest spot) is found in the section containing the position of the sun at its maximal elevation ($\approx 67^\circ$ at the given latitude). Only diffuse radiation is incident from inclination angles above 67° . The direct component causes a shift in the distribution toward higher inclination angles (Figure 2B). The median angle, defined so that equal parts (50%) of the total radiation are received from smaller and larger inclination angles, respectively, was 37.6° . For comparison, the median angle of isotropic radiation is 30° .

The angular distribution of PAR becomes narrower and its center (the median angle) moves closer to the zenith with depth in the canopy (Figure 4), because near-horizontal angles get rapidly blocked (see Figure 3A). However, even in the lower canopy, the radiation was incident from many different directions (Figures 3B and 4A).

Shoot and needle structure versus canopy openness

Interpolation surfaces for SSA were fairly symmetrical with respect to the γ -axis but somewhat skewed in the ϕ -direction (Figure 1). In sun shoots, where needles point upward, the shoot silhouette area is significantly larger when the shoot is viewed from the base toward the tip (i.e., for negative values of ϕ). Accordingly, maximum SSA was generally not obtained at $\phi = 0^\circ$, but at slightly negative ϕ -values. Shade shoots are flatter than sun shoots, which implies a larger variation in SSA along the γ -axis. The sun shoot depicted in Figure 1 had $SPAR_{max} = 0.422$ and $\overline{SPAR} = 0.292$. Values for the shade shoot were $SPAR_{max} = 0.644$ and $\overline{SPAR} = 0.412$.

Both \overline{SPAR} and $SPAR_{max}$ decreased with canopy openness, which ranged from 0.006 to 0.82 (Figure 5, Table 1). Moderate shading had only a small effect on SPAR, whereas a sharp increase occurred in deeper shade (openness ≈ 0 –25%). There

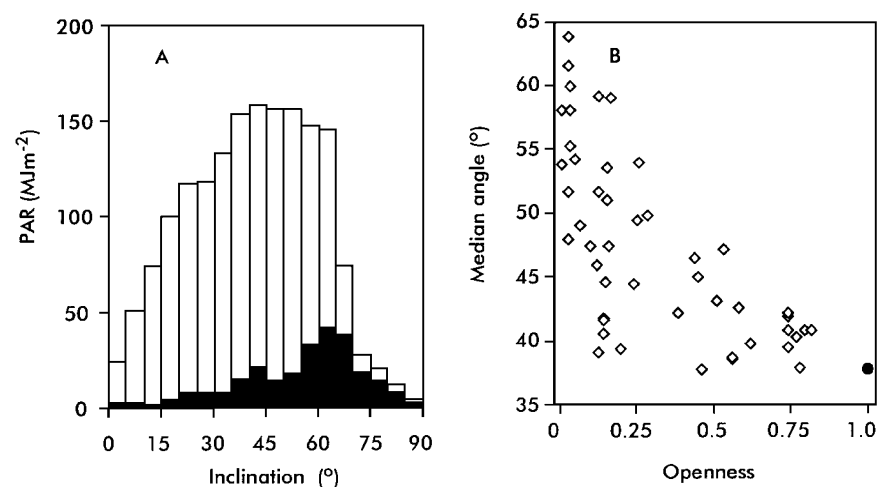


Figure 4. A. Energy of PAR during growing season incident from different inclination angles at the locations of the sun shoot (\square) and shade shoot (\blacksquare). B. The median angle of incident radiation for all sample shoots plotted against canopy openness. The \bullet denotes the median angle (36.6°) of above-canopy radiation (canopy openness = 1).

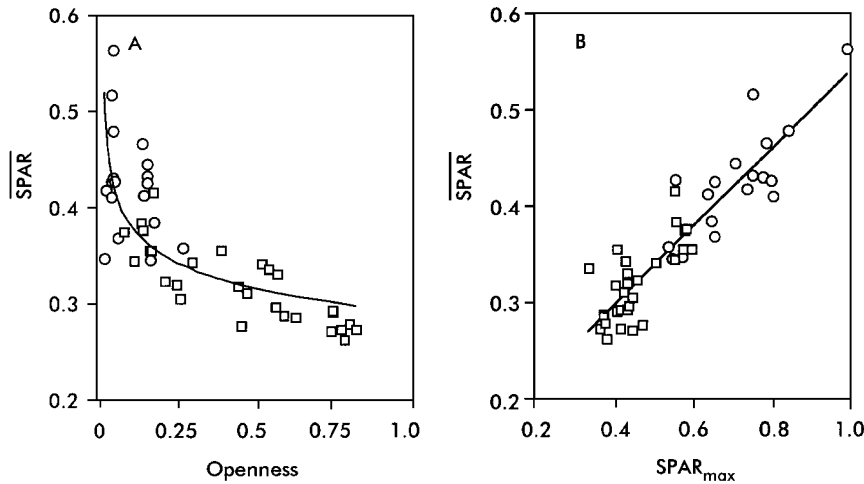


Figure 5. A. Relationship between $\overline{\text{SPAR}}$ and canopy openness. B. Relationship between SPAR_{max} and $\overline{\text{SPAR}}$. Symbols: dominant and codominant trees (tree height > 6 m) are represented by \square ; intermediate and suppressed trees (tree height < 6 m) by \circ . Regressions fitted to whole data: A. $r^2 = 0.59$ and B. $r^2 = 0.83$.

was a strong linear correlation ($r^2 = 0.83$) between SPAR_{max} and $\overline{\text{SPAR}}$ (Figure 5B); however, SPAR_{max} increased relatively more with shading than did $\overline{\text{SPAR}}$. Mean SPAR_{max} for the five most sunlit shoots (mean openness = 0.784) was 0.395, and for the five most shaded shoots (mean openness = 0.020), it was 0.737, i.e., 1.86 times greater. The corresponding values for $\overline{\text{SPAR}}$ were 0.275 and 0.424, giving a ratio of 1.54.

Needle thickness increased and specific needle area (SNA) decreased with canopy openness (Figure 6). As a result of changes in $\overline{\text{SPAR}}$ (Figure 5) and SNA, mean shoot silhouette area per unit needle mass dry weight (ndw) $\overline{\text{SSA}}/\text{ndw}$ (= the product of $\overline{\text{SPAR}}$ and SNA) was up to five times higher for shade shoots than for sun shoots (Figure 6C).

Needle nitrogen concentration increased with canopy openness in the dominant and codominant trees, but in the suppressed and intermediate trees, this relationship broke down (Figure 7A). The highest nitrogen concentrations were found in needles from suppressed trees. As a result, there was no correlation between nitrogen concentration and canopy openness for the data as a whole (all trees). A strong positive correlation, on the other hand, existed between nitrogen content per unit projected needle area and canopy openness (Figure 7B).

Efficiency of light capture

The SLI/SLI_0 ratio varied between 0.25 to 0.76, and showed a strong negative nonlinear correlation ($r^2 = 0.67$) with canopy

openness (Figure 8). The lower curve depicted in Figure 8 shows the corresponding value of $\overline{\text{SPAR}}$. There was a strong linear correlation ($r^2 = 0.99$) between SLI/SLI_0 and $\overline{\text{SPAR}}$, but SLI/SLI_0 was, on average, 15% higher. If there was no directional variation in either SPAR or in the radiation field surrounding the shoot, SLI/SLI_0 would be equal to $\overline{\text{SPAR}}$. The difference may be interpreted as the increase in SLI caused by a favorable orientation of the shoot in relation to the actual radiation field at its location.

Distribution of light and nitrogen

Nitrogen content was linearly related to SLI (Figure 9), but the regression line had a positive intercept because the ratio of nitrogen to intercepted PAR increased toward the bottom of the canopy. Although (as a result of the changes in shoot geometry) the total range of variation in SLI (0.94 to 59.5 kJ cm^{-2}) was considerably less than the total range in canopy openness, it remained many times greater than the variation in nitrogen content (0.084 to 0.354 mg cm^{-2}). Consequently, proportionality between these two variables could not be expected. For the whole data, there was a more than twentyfold variation (38.8 to 980.8 mg kJ^{-1}) in the ratio of nitrogen to intercepted PAR. The largest ratios and most of the variation occurred in the lower canopy. For shoots situated at a canopy openness above 30%, the range of variation in the amount of nitrogen per unit of intercepted PAR was reduced to between 38.8 and

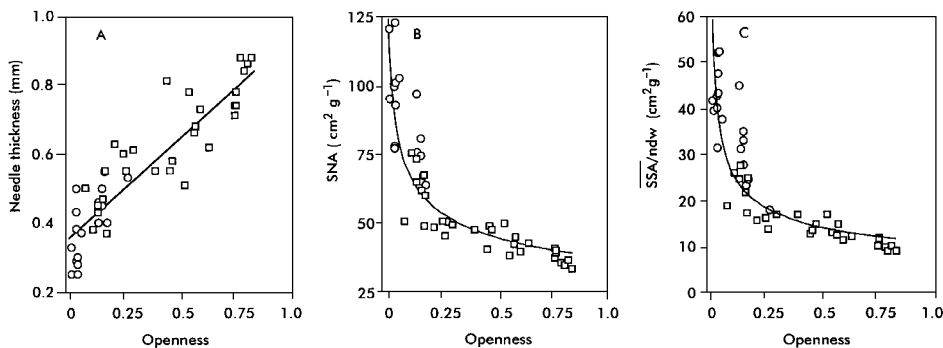


Figure 6. Needle thickness, SNA, and SSA/ndw as a function of canopy openness (symbols are as in Figure 5). Regressions: A. $r^2 = 0.81$; B. $r^2 = 0.82$; and C. $r^2 = 0.82$.

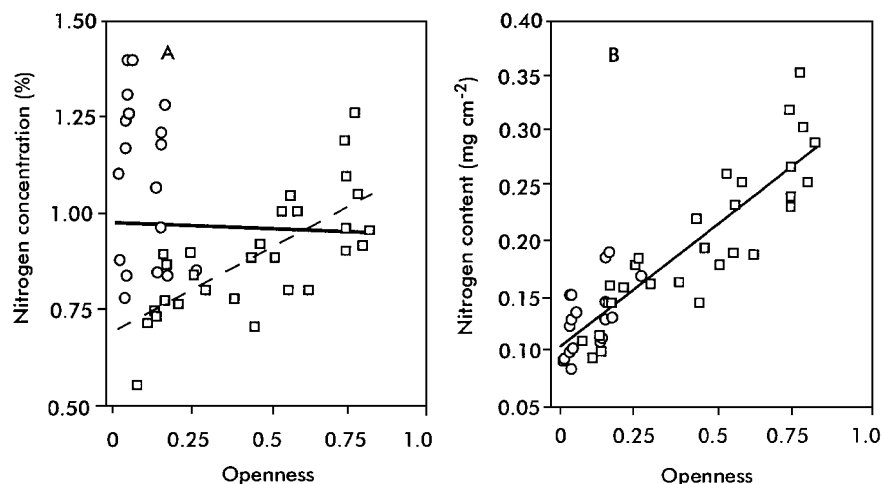


Figure 7. A. Relationship between nitrogen concentration and canopy openness. Thick line = all trees ($r^2 = 0.002$); thin line = dominant and codominant trees ($r^2 = 0.52$). B. Relationship between nitrogen content and canopy openness ($r^2 = 0.80$). Symbols: dominant and codominant trees (tree height > 6 m) are represented by \square ; intermediate and suppressed trees (tree height < 6 m) by \circ .

72.0 mg kJ^{-1} , and no correlation ($r^2 = 0.004$) of the ratio with canopy openness remained.

Discussion

Shade acclimation and light interception efficiency

The ratio SLI/SLI_0 , which was used to quantify the efficiency of light capture by shoots in the prevailing light conditions, was more than twice as high in shade shoots as in sun shoots (Figure 8). The increase in SLI/SLI_0 with shading is consistent with an efficient utilization of light by the canopy as a whole. Efficient light capture is not necessarily useful at the top of the canopy, where there is more than enough light available to maintain high rates of photosynthesis. On the contrary, low light-capturing efficiency of sun shoots may be advantageous because it implies a reduced risk of light saturation and smaller

transpiration demand (because the intercepted light is distributed over a large leaf area). Moreover, it enables more light to penetrate to deeper canopy layers, thus improving the light conditions of shade shoots. This, in combination with the high light-capturing efficiency of shade shoots, considerably evens out the vertical gradient in intercepted light (Stenberg 1996).

The increase in SLI/SLI_0 with shading was mainly achieved by smaller within-shoot shading (larger $\overline{\text{SPAR}}$) in shade shoots than in sun shoots (Figure 5). In addition, the combined effects of shoot orientation and variation in SSA acted to increase SLI of a shoot in its prevailing (non-isotropic) light conditions. The SLI was, on average, about 15% higher than would be predicted simply by the increase in $\overline{\text{SPAR}}$ (Figure 8), indicating a tendency of the shoots to be oriented so as to increase their light interception. However, the increase in SLI caused by a favorable shoot orientation was modest and not appreciably higher for shade shoots than for sun shoots. This is because

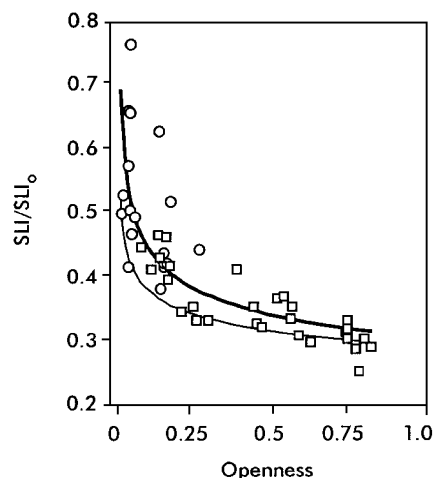


Figure 8. Ratio of SLI to SLI_0 as a function of canopy openness. The lower curve (thin line) shows the value of $\overline{\text{SPAR}}$ (Figure 5A). Symbols: dominant and codominant trees (tree height > 6 m) are represented by \square ; intermediate and suppressed trees (tree height < 6 m) by \circ .

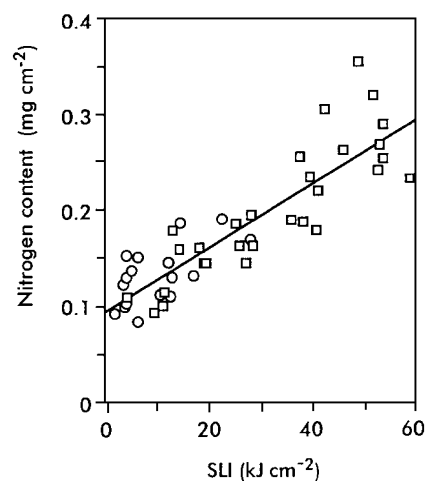


Figure 9. Relationship between nitrogen content and SLI. The regression line is: $y = 0.0032x + 0.097$; $r^2 = 0.78$. Symbols: dominant and codominant trees (tree height > 6 m) are represented by \square ; intermediate and suppressed trees (tree height < 6 m) by \circ .

even in the lower canopy, the angular distribution of PAR is not concentrated around one particular direction (Figures 3 and 4). Thus, the "optimal solution," represented by a flat shoot turning its maximal silhouette area perpendicular to the (one) direction of radiation, cannot be realized.

Differences in needle shape cause some ambiguity in the interpretation of SLI, when SLI is defined on a projected needle area basis. Because sun needles are thicker than shade needles (Figure 6), they have a larger ratio of total to projected area. Consequently, the difference in SLI/SLI_0 between sun and shade shoots would have been larger if SLI had been expressed on a total needle area basis. The same is true, only to a much larger extent, when the efficiency of light interception is expressed on a needle mass basis. Because of the increase in SNA with shading, mean silhouette area per unit needle dry weight (\overline{SSA}/ndw) was up to five times higher in shade shoots than in sun shoots (Figure 6).

Relation between nitrogen and intercepted light

Changes in shoot geometry brought about a considerable flattening of the vertical gradient of light interception per unit needle area (SLI). The increase in specific needle area (SNA) with shading (Figure 6) further decreased the differences in light interception by sun and shade shoots, when expressed per unit needle mass. However, because mean nitrogen concentration was similar in shade needles and sun needles (Figure 7), the amount of nitrogen per unit intercepted PAR was much higher at the bottom of the canopy than at the top of the canopy (Figure 9).

Conclusions

To develop and test theories on the optimal use of resources, we need accurate estimates of how these resources are allocated in real canopies. It has proved particularly problematic to measure the amount of intercepted PAR by leaves at different positions in the canopy. Technical difficulties arise from the great temporal and spatial variation of irradiance that occurs in the canopy. A far more serious problem, however, is the lack of correspondence between PAR measured with artificial surfaces (e.g., flat horizontally lying sensors) and the distribution of PAR on the actual needle surface. As shown in this study, within-shoot shading and variation in leaf angle and shoot shape greatly modify the gradient of light interception within the canopy.

To estimate quantitatively light interception by a shoot, the directional distributions of SSA and PAR incident on the shoot must be known. The directional distribution of above-canopy PAR at any given location can be produced in a straightforward manner. It can then be combined with hemispherical photographs (or measurements with the LAI-2000 plant canopy analyzer; Li-Cor, Inc., Lincoln, NE) to give the directional distribution of PAR and an estimate of SLI_0 at any desired (shoot) location in the canopy.

The method applied here to produce the directional distribution of shoot silhouette area is too cumbersome for standard use. However, the interpolation surfaces (Figure 1) constructed

in this exercise indicate that there is a high degree of regularity in the shoot shape, which was also supported by the strong correlation between \overline{SPAR} and $SPAR_{max}$ (Figure 5B). It seems reasonable to believe, therefore, that the directional distribution of shoot silhouette area could be estimated fairly accurately using a shape function based on measurements in a few specified directions only (Stenberg 1996). This would offer an operational method for the determination of seasonal light interception by shoots at different positions in the canopy, not involving any measurements of irradiance.

A close correlation was found between \overline{SPAR} and the light-capturing efficiency (SLI/SLI_0). The SLI/SLI_0 was higher than predicted by \overline{SPAR} alone (Figure 8), but the gradients were similar. Thus, if actual values of SLI are not needed, \overline{SPAR} combined with the radiation regime may provide a good estimate of the gradient of light interception (relative difference at top and bottom of the canopy). To simplify further, the close dependency between \overline{SPAR} and $SPAR_{max}$ makes it possible to estimate \overline{SPAR} based on measurements of $SPAR_{max}$.

Acknowledgments

This work was supported by a grant from the Finnish Academy of Science to H. Smolander. The authors express sincere thanks to Thomas M. Hinckley and Timothy A. Martin for help in field measurements and use of the OPTIMAS-system, and to Pekka Voipio for assistance with data processing and figures.

References

- Anderson, M.C. 1964. Studies of the woodland light climate. I. The photographic computation of light conditions. *J. Ecol.* 52:27–41.
- Bloom, A.J., F.S. Chapin and H.A. Mooney. 1985. Resource limitation in plants—an economic analogy. *Annu. Rev. Ecol. Syst.* 16:363–392.
- Chen, J.-L., J.F. Reynolds, P.C. Harley and J.D. Tenhunen. 1993. Coordination theory of leaf nitrogen distribution in a canopy. *Oecologia* 93:63–69.
- Ellsworth, D.S. and P.B. Reich. 1993. Canopy structure and vertical patterns of photosynthesis and related leaf traits in a deciduous forest. *Oecologia* 96:169–178.
- Evans, J.R. 1989. Photosynthesis and nitrogen relationships in leaves of C_3 plants. *Oecologia* 78:9–19.
- Evans, J.R. 1993. Photosynthetic acclimation and nitrogen partitioning within a lucerne canopy. I. Canopy characteristics. *Aust. J. Plant Physiol.* 20:55–67.
- Farquhar, G.D. 1989. Models of integrated photosynthesis of cells and leaves. *Phil. Trans. R. Soc. Lond.* 323:357–367.
- Field, C.B. 1983. Allocating leaf nitrogen for the maximization of carbon gain: leaf age as a control on the allocation program. *Oecologia* 56:341–347.
- Field, C.B. and H.A. Mooney. 1986. The photosynthesis–nitrogen relationship in wild plants. *In* *On the Economy of Plant Form and Function*. Ed. T. Givnish. Cambridge Univ. Press, Cambridge, pp 25–55.
- Fritschen, L.J. and J. Hsia. 1979. Estimation of hourly direct beam and diffuse solar radiation from global solar radiation measurements. *In* *Proc. Solar '79 Northwest*. Eds. S. King and S. Killen. Solar 1979 Northwest, Seattle, WA, pp 193–194.
- Hirose, T., M.J.A. Werger and J.W.A. van Rheenen. 1989. Canopy development and leaf nitrogen distribution in a stand of *Carex acutiformis*. *Ecology* 70:1610–1618.

- Hollinger, D.Y. 1989. Canopy organization and foliage photosynthetic capacity in a broad-leaved evergreen montane forest. *Func. Ecol.* 3:53–62.
- Horn, H. 1971. The adaptive geometry of trees. Princeton Univ. Press, Princeton, NJ, 144 p.
- Kershaw, J.A. and D.R. Larsen. 1992. A rapid technique for recording and measuring the leaf area conifer needle samples. *Tree Physiol.* 11:411–417.
- Kull, O. and Ü. Niinemets. 1993. Variations in leaf morphometry and nitrogen concentration in *Betula pendula*, *Corylus avellana*, and *Lonicera xylosteum*. *Tree Physiol.* 12:311–318.
- Kuroiwa, S. 1970. Total photosynthesis of a foliage in relation to inclination of leaves. In Prediction and Measurement of Photosynthetic Productivity. Ed. I. Setlik. Proc. IBP/PP Tech. Meeting, Trebon. Ctr. for Agric. Publishing and Documentation, Wageningen, The Netherlands, pp 79–89.
- Leverenz, J.W. and T.M. Hinckley. 1990. Shoot structure, leaf area index, and productivity of evergreen conifer stands. *Tree Physiol.* 6:135–149.
- Miller, P.C. 1967. Leaf temperature, leaf orientation, and energy exchange in quaking aspen (*Populus tremuloides*) and Gambell's oak (*Quercus gambellii*) in central Colorado. *Oecol. Plant.* 2:241–270.
- Mooney, H.A. and S.L. Gulmon. 1979. Environmental and evolutionary constraints on the photosynthetic characteristics of higher plants. In Topics in Plant Population Biology. Eds. O.T. Solbrig, S. Jain, G.B. Johnson and P. Raven. Cambridge Univ. Press, NY, pp 316–337.
- Niinemets, Ü. and O. Kull. 1995. Effects of light availability and tree size on the architecture of assimilative surface in the canopy of *Picea abies*: variation in needle morphology. *Tree Physiol.* 15:307–315.
- Oker-Blom, P. and H. Smolander. 1988. The ratio of shoot silhouette area to total needle area in Scots pine. *For. Sci.* 34:894–906.
- Press, W.H., S.A. Teukolsky, W.T. Vetterling and B.P. Flannery. 1992. Numerical recipes in FORTRAN, 2nd Edn. Cambridge Univ. Press, 963 p.
- Rich, P.M. 1989. A manual for analysis of hemispherical canopy photography. Los Alamos National Laboratory, LA-11733-M. Los Alamos, NM, 80 p.
- Sprugel, D.G. 1989. The relationship of evergreenness, crown architecture, and leaf size. *Am. Nat.* 133:465–479.
- Sprugel, D.G., J.R. Brooks and T.M. Hinckley. 1996. Effect of light on shoot geometry and needle morphology in *Abies amabilis*. *Tree Physiol.* 16:91–98.
- Stenberg, P. 1996. Simulations of the effect of shoot structure and orientation on vertical gradients in intercepted light by conifers. *Tree Physiol.* 16:99–108.
- Stenberg, P., S. Linder and H. Smolander. 1995. Variation in the ratio of shoot silhouette area to needle area in fertilized and non-fertilized trees of Norway spruce. *Tree Physiol.* 15:705–712.
- Verhagen, A.M.W., J.H. Wilson and E.J. Britten. 1963. Plant production in relation to foliage illumination. *Ann. Bot.* 27:627–640.
- Weiss, A. and J.M. Norman. 1985. Partitioning solar radiation into direct and diffuse, visible and near-infrared components. *Agric. For. Meteorol.* 34:205–213.
- Western Solar Utilization Network. 1980. Washington solar and weather information: one in a series of thirteen climate data manuals for the states of the Western Region. Western SUN, Portland, OR, 43 p.

